

Location of the TEMPO moiety of TEMPO-PC in phosphatidylcholine bilayers is membrane phase dependent

Seonghoon Kim¹ and Changbong Hyeon^{1,*}

¹School of Computational Sciences, Korea Institute for Advanced Study, Seoul, Korea

ABSTRACT The (2,2,6,6-tetramethylpiperidin-1-yl)oxyl (TEMPO) moiety tethered to the headgroup of phosphatidylcholine (PC) lipid is employed in spin labeling electron paramagnetic resonance spectroscopy to probe the water dynamics near lipid bilayer interfaces. Due to its amphiphilic character, however, TEMPO spin label could partition between aqueous and lipid phases, and may even be stabilized in the lipid phase. Accurate assessment of the TEMPO-PC configuration in bilayer membranes is essential for correctly interpreting the data from measurements. Here, we carry out all-atom molecular dynamics (MD) simulations of TEMPO-PC probe in single-component lipid bilayers at varying temperatures, using two standard MD force fields. We find that, for a dipalmitoylphosphatidylcholine (DPPC) membrane whose gel-to-fluid lipid phase transition occurs at 314 K, while the TEMPO spin label is stabilized above the bilayer interface in the gel phase, there is a preferential location of TEMPO below the membrane interface in the fluid phase. For bilayers made of unsaturated lipids, 1,2-Dioleoyl-sn-glycero-3-phosphocholine (DOPC) and 1-palmitoyl-2-oleoyl-sn-glycero-3-phosphocholine (POPC), which adopt the fluid phase at ambient temperature, TEMPO is unequivocally stabilized inside the bilayers. Our finding of membrane phase-dependent positioning of the TEMPO moiety highlights the importance of assessing the packing order and fluidity of lipids under a given measurement condition.

SIGNIFICANCE We find that TEMPO-PC changes its configuration depending on the phase of bilayer membrane. When bilayer membranes are in gel phase below melting temperature, TEMPO moiety is stabilized above the bilayer interface, probing the lipid/water interface. In contrast, when the membranes are in fluid phase, TEMPO is stabilized inside the bilayer, probing the upper part of hydrocarbon tails. Our study underscores the importance of assessing the physico-chemical condition of bilayer membranes in properly interpreting the data collected from TEMPO-PC.

INTRODUCTION

TEMPO ((2,2,6,6-tetramethylpiperidin-1-yl)oxyl) is a six-membered cyclic nitroxide radical shielded by four methyl groups. Tethered at various positions along the hydrocarbon tail in the form of *n*-doxyl phosphatidylcholine (PC) lipids, nitroxide spin labels, including TEMPO, have been employed to measure the penetration depth of solvent molecules and the flexibility of lipid tail by analyzing homogeneous line broadening of electron paramagnetic resonance (EPR) spectra (1–4) and fluorescence quenching (5,6). Meanwhile, TEMPO-PC, a molecular construct in which TEMPO molecule is tethered to the choline group of PC, has been used to probe the water/lipid interfacial mo-

lecular environment (7–9) with an estimate based on a molecular model that TEMPO is positioned at 5 Å above the bilayer interface (10–12).

The location of the TEMPO moiety in PC bilayers is, however, not entirely clear and remains controversial in the recent literature. A series of molecular dynamics (MD) simulation and fluorescence quenching-based studies have been showing that PC headgroup-labeled probes, e.g., 1,6-diphenyl-1,3,5-hexatriene, 7-nitrobenz-2-oxa-1,3-diazol-4-yl (NBD), and TEMPO, reside in the acyl chain region (13–18). In contrast, indirect EPR relaxation data (19) have been interpreted as evidence that headgroup-labeled TEMPO resides in the aqueous phase, protruded at ~ 5 Å above the bilayer interface.

Here, we investigate the location of TEMPO spin label of TEMPO-PC in PC bilayers by carrying out a set of careful simulations. We first perform brute-force MD simulations at different temperatures to get rough ideas on the location

Submitted March 25, 2022, and accepted for publication May 26, 2022.

*Correspondence: hyeoncb@kias.re.kr

Editor: H. Raghuraman.

<https://doi.org/10.1016/j.bpj.2022.05.044>

© 2022 Biophysical Society.

of the TEMPO moiety in DPPC bilayers, and next determine a thermodynamically more reliable location of TEMPO by calculating the potential of mean forces (PMFs) via the umbrella sampling method. PMFs of the TEMPO moiety in *unsaturated* PC bilayers (DOPC, POPC) are also calculated. The PMFs obtained with three lipid types at varying temperatures using two different MD force fields allow us to draw a general conclusion that the location of the TEMPO moiety is membrane phase dependent. To be specific, if the bilayers are in fluid phase, TEMPO-PC adopts a configuration in which the TEMPO group is stabilized inside bilayers (TEMPO-in configuration), whereas if the bilayers are in gel phase, TEMPO-PC adopts the TEMPO-out configuration, in which the TEMPO group is stabilized above the lipid-water interface.

METHODS

Preparation of systems and analysis

We modeled TEMPO-PC by assembling TEMPO and DPPC using the CHARMM36 force field (20,21). Four TEMPO-PCs were placed (two TEMPO-PCs in each leaflet) in the DPPC bilayer (64 lipids in each leaflet) and assembled with 150 mM NaCl ions (15 Na⁺ and 15 Cl⁻) and SPC water models filling the remaining space of the simulation box. The membrane assembly, necessary input files, force field format conversion, and simulation protocols were set up by employing the CHARMM-GUI Membrane Builder (22). All simulations were performed using GROMACS 2020.4 (23). The origin of the system was set to the center of an $L_x \times L_y \times L_z$ periodic box ($L_x = L_y \approx 65$ Å, $L_z \approx 90$ Å). After minimizing the energy of the system using the steepest descent algorithm, the system was equilibrated for ~ 2 ns by gradually reducing the positional and dihedral restraints on the lipids. In the equilibration step, we first gradually heated up the energy-minimized DPPC bilayer systems to our target temperature with 0.3–3 K/ns and equilibrated them in the NVT ensemble with a 1-fs integration time step, followed by that in the NPT ensemble at $P = 1$ bar with a 2-fs time step. The 500-ns production runs in the NPT ensemble were generated at each temperature over the temperature range $T = (260\text{--}330$ K). The semi-isotropic Parrinello-Rahman method and a Nosé-Hoover thermostat were employed to realize the conditions of the constant pressure and temperature. The bond lengths involving hydrogen atoms were constrained using the LINCS algorithm. Area per lipid (A), bilayer thickness (D_{HH}), and density profiles along the bilayer depth were calculated using the last 200 ns of the simulation trajectory. In the NPT ensemble, the A was calculated by dividing the area of the simulation box in the xy direction with the number of lipids in one of the leaflets (66 lipids = 64 DPPC + 2 TEMPO-PC). In addition, the D_{HH} was calculated by taking the average over the z values between the phosphorus atoms of the lipids in the upper and lower leaflets.

PMF calculation

The umbrella sampling was performed to calculate the PMF of TEMPO along the DPPC bilayer at $T = (290\text{--}320$ K). To eliminate intermolecular interaction between TEMPO moieties, only a single TEMPO-PC was placed in each leaflet. Using the last snapshot of the foregoing MD simulation as the initial configuration, we pulled the oxygen atom of the TEMPO in each leaflet along the z axis using a harmonic potential with stiffness constant $k = 100$ kJ mol⁻¹ Å⁻². In total, 31 sampling windows with 1 Å sized bins were placed over $0 \text{ Å} \leq |z| \leq 30 \text{ Å}$. After 100 ps equilibration with $k = 100$ kJ mol⁻¹ Å⁻² positional restraint, umbrella sampling was conducted for 5 ns at each bin with the umbrella stiffness $k = 35$ kJ mol⁻¹

Å⁻² using PLUMED (24,25). A weighted histogram analysis method was used to combine the results from all the windows to build the PMF of TEMPO. The position of the phosphorus atom within ± 10 Å in the xy -plane from the oxygen radical of the TEMPO moiety was set to $\Delta z = 0$ of the PMF. Finally, the PMFs were obtained by averaging over all the five replicas.

PMF calculation was also repeated in DOPC and POPC bilayers at $T = 310$ K under CHARMM36 (20,21) and AMBER Lipid17 (unpublished data). For the case of AMBER Lipid17, we adopted the TEMPO model by Stendardo et al. (26).

RESULTS

TEMPO-PC in DPPC bilayers at varying temperatures

We first carry out a series of 500 ns brute-force MD simulations of a fully hydrated DPPC bilayer system containing ~ 3 mol % TEMPO-PC at varying temperatures by using the CHARMM36 force field. The snapshots of simulation visualize how the configurations of lipid bilayer and TEMPO-PC change with temperature (Fig. 1 A). At high temperatures ($T = 320, 330$ K), the bilayer membrane adopts a fluid phase, and the TEMPO-PC adopts the TEMPO-in configuration, such that the TEMPO moiety is stabilized inside the bilayer interface. At low temperatures, especially in the range of $290 \text{ K} \leq T \leq 310$ K, the acyl chains of lipids adopt ordered configuration, and partial overlaps between the upper and lower leaflets give rise to corrugation in the bilayer surface, reminiscent of the $P_{\beta'}$ (ripple) phase (28,29). TEMPO-in and TEMPO-out configurations coexist in this temperature range, yielding the bimodal distributions in the TEMPO location normal to the membrane. At even lower temperature ($T = 260$ and 270 K), the TEMPO-out configuration becomes dominant (Fig. 1 A).

The two key physical characteristics of the DPPC bilayers, area per lipid (A) and bilayer thickness (D_{HH}), the latter of which measures the average distance between the phosphate groups in the upper and lower leaflets are in reasonable agreement with experimental measurements (filled circles in *magenta* and *cyan* in Fig. 1 B). From $A(T)$ and $D_{\text{HH}}(T)$, the gel-to-fluid (or P_{β} -to- L_{α}) lipid phase transition temperature ($T_m = 314$ K) is correctly identified (27,30–34).

PMF of TEMPO spin label in DPPC bilayers

In the foregoing result from the brute-force MD simulations, simulation time may not be long enough to give thermodynamically reliable results. The simulations offer only a rough idea of TEMPO-PC configurations. To determine the temperature-dependent configuration of TEMPO-PC in the DPPC bilayers, we carry out the umbrella sampling to calculate the PMF of the TEMPO group across the DPPC bilayer using two standard force fields, CHARMM36 and AMBER LIPID17. To avert the possibility that two different

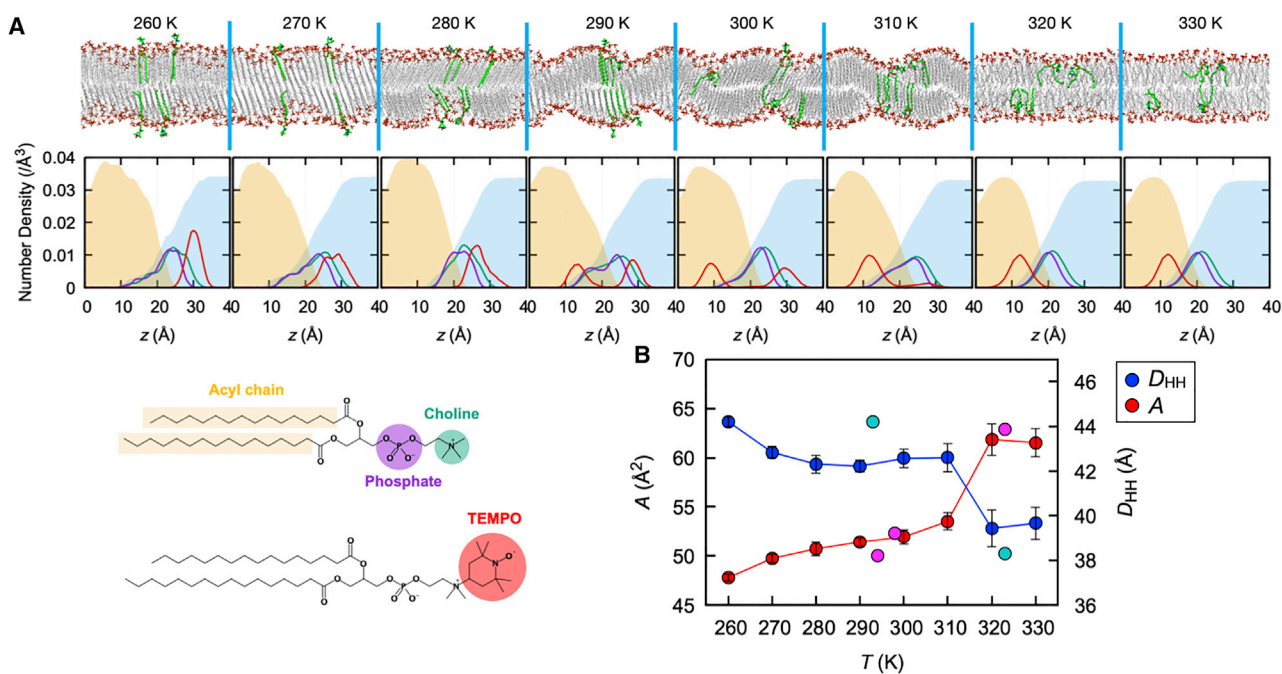


FIGURE 1 MD simulations of TEMPO-PC in DPPC bilayers at varying temperatures. (A) Snapshots of TEMPO-PC configurations in DPPC bilayers (first row). The density profiles of the heavy atoms in phosphate (magenta) and choline groups (green) and TEMPO (red) are shown in the second row, along with acyl chain in DPPC (filled ivory), and water (filled pale blue). The density of the TEMPO moiety (red) is amplified by fivefold for clarity. (B) Area per lipid (A) and bilayer thickness (D_{HH}) of DPPC bilayers at varying temperatures (error bars denote the standard deviation) obtained from MD simulations under the CHARMM36 force field. The filled circles in magenta and cyan represent the measurements (27) for A and D_{HH} , respectively. The gel-to-fluid phase transition temperature of DPPC membranes is estimated to be $T_m = 314$ K from the crossing point of A and D_{HH} . See Fig. S1 for the result obtained under an AMBER LIPID17 force field. To see this figure in color, go online.

TEMPO-PCs in the same leaflet interact with each other and compromise our PMF calculation, we place only a single TEMPO-PC in each leaflet, effectively making a system of DPPC bilayers containing ~ 1.5 mol % TEMPO-PC.

Because of substantial fluctuations, corrugation of bilayer interface, and the temperature-dependent membrane thickness (Fig. 1 A), the distance from the bilayer center is not a convenient metric to discuss whether the TEMPO moiety is in the interior or exterior of the bilayer interface. Thus, for straightforward determination of the TEMPO location, we set the average position of phosphate group as the reference penetration depth ($\Delta z = 0$) of TEMPO, so that we can easily assess from PMF whether the TEMPO-PC adopts TEMPO-in ($\Delta z < 0$) or TEMPO-out ($\Delta z > 0$) configuration. In addition, we monitor the minimal distance (d_{TA}) between the methyl groups of TEMPO and the upper part of the hydrocarbon tail (C2-C5 of acyl groups) as another coordinate to characterize the TEMPO-PC configuration. The two-dimensional (2D) PMFs calculated as a function of Δz and d_{TA} (Fig. 2) demonstrates that the dominant population of the TEMPO-PC configuration is formed at $\Delta z = 5$ Å and $d_{TA} \approx (8 - 12)$ Å at $T = 290$ K, and at -10 Å $< \Delta z < -5$ Å and $d_{TA} \approx (3 - 4)$ Å at $T = 320$ K. The former denotes the TEMPO-out configuration; more specifically, the TEMPO moiety is stabilized in the aqueous phase, being excluded from the compactly ordered lipid phase. On the

other hand, in the latter configuration (-10 Å $< \Delta z < -5$ Å and $d_{TA} \approx (3 - 4)$ Å), TEMPO-PC adopts bent configurations in which the TEMPO group is stabilized in the lipid phase.

1D projection of 2D PMF in Fig. 2 leads to the 1D PMFs demonstrated in Fig. 3. The results obtained using the AMBER LIPID17 force field reconfirm that the TEMPO group is stabilized at $\Delta z \sim 5$ Å, i.e., above the bilayer interface of the DPPC membrane at $T = 290$ K, so that the TEMPO-out configuration becomes dominant (Fig. 3 A). In contrast, at $T = 300, 310,$ and 320 K, TEMPO is stabilized at the penetration depth of -10 Å $< \Delta z < -5$ Å with free energy bias of $\sim (5 - 7) k_B T$ toward the lipid phase (Fig. 3 A). The 1D PMFs under CHARMM36 yield a similar tendency, except for $T = 300$ K at which the TEMPO-out configuration is favored (Fig. 3 B). We note that T_m estimated for the DPPC bilayers under AMBER LIPID17 is lower than the value under CHARMM36 by ~ 10 K (compare Fig. S1 B with Fig. 1 B).

PMFs of TEMPO spin label in unsaturated lipid bilayers

Bilayers formed from unsaturated lipids, such as POPC and DOPC, characterized with low lipid phase transition temperature ($T_m \approx -2^\circ\text{C}$ for POPC (35,36) and $T_m \approx -16.5^\circ\text{C}$

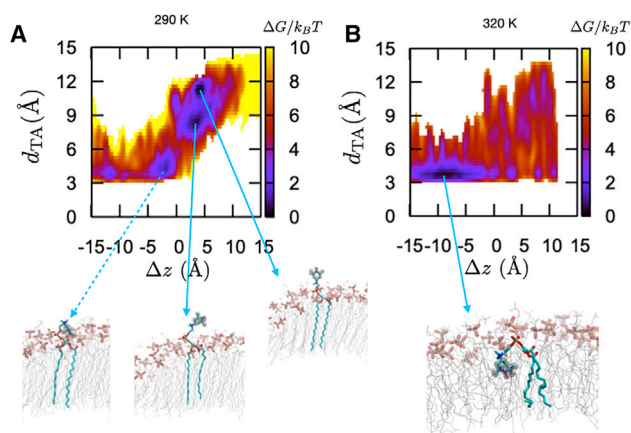


FIGURE 2 2D PMF of TEMPO spin label in the DPPC bilayers calculated as a function of Δz (height difference between nitroxide oxygen and phosphorus atoms) and d_{TA} (minimal distance between any heavy atom of TEMPO and C2-C5 of acyl chain at (A) $T = 290$ K) and (B) $T = 320$ K). Depicted are the snapshots of TEMPO-PC configuration at free energy minima with phosphate groups of DPPC visualizing the lipid-water interface. TEMPO-out and TEMPO-in configurations are dominant at $T < T_m$ and $T > T_m$, respectively. The calculation was carried out under AMBER LIPID17. See Fig. S2 for the 2D PMFs obtained under the CHARMM36 force field. To see this figure in color, go online.

for DOPC (37)), are in the fluid phase at ambient temperature. We repeated the PMF calculation of the TEMPO spin label along the Δz axis in POPC and DOPC membranes at $T = 310$ K using the two force fields (Fig. 4). Besides the variations with lipid types and force fields, the PMFs of TEMPO unequivocally indicate that the TEMPO-in configuration is more favorable. The thermodynamically favorable position of TEMPO at $-10 \leq \Delta z \leq -5$ Å with a free energy bias of $(5 - 7) k_B T$ is consistent with our previous MD simulation

study of TEMPO-PC in POPC bilayers modeled with Berger force field (16).

DISCUSSION

Here, we discuss our key finding of membrane phase-dependent location of the TEMPO moiety in light of historical perspective, current observations, and the questions raised over the past years.

- 1) It has been known from earlier studies in the 1970s that unsubstituted TEMPO molecules can partition between fluid hydrophobic regions of lipids and the aqueous region (38). The partition coefficient or the solubility of TEMPO to the lipid phase increases with the fluidity of the lipids, whereas it is excluded from paracrystalline regions (gel phase) of lipid bilayers (38). Thus, an empirical relationship between the partition coefficient of TEMPO and the lipid order parameter determined with EPR signals (A_{\parallel} outer hyperfine splitting) from TEMPO-labeled fatty acid (say, 5-PC) allows one to determine the fraction of lipid in the fluid phase membrane (38,39), enabling construction of the phase diagram of phospholipid mixtures (40,41).

A certain difference may exist between the molecular behaviors of the unsubstituted TEMPO and the TEMPO moiety attached to PC headgroup in bilayer membranes. However, the TEMPO-labeled headgroup is flexible and subject to larger thermal fluctuations. It is noteworthy that fluctuations of the TEMPO moiety buried inside the membrane at $T > T_m$ are still larger than the fluctuations of TEMPO residing in the aqueous phase at $T < T_m$. Fluctuations in the TEMPO position increase gradually with

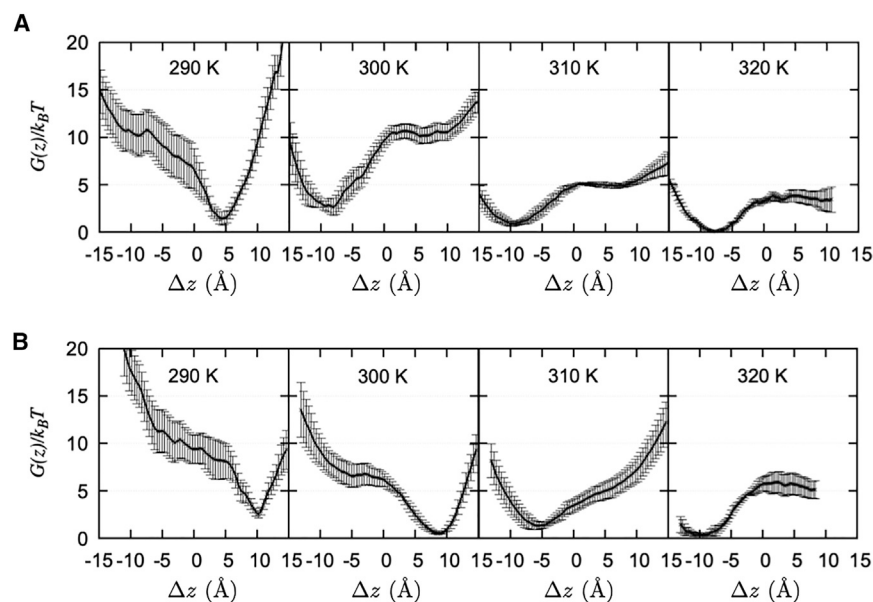


FIGURE 3 PMFs of TEMPO spin label (nitroxide oxygen) in the DPPC bilayers at various temperatures (error bars are estimated standard error) calculated using the (A) AMBER Lipid17 and (B) CHARMM36 force fields.

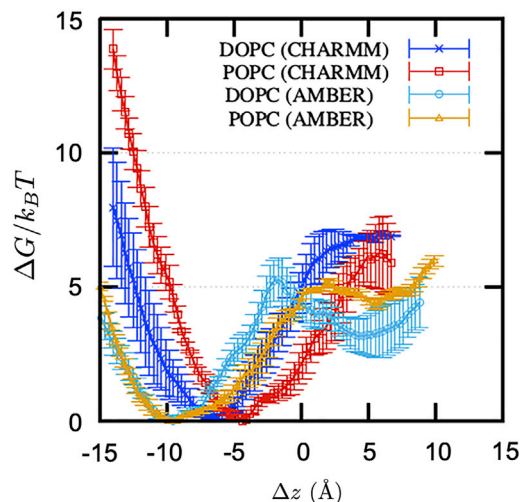


FIGURE 4 PMFs of TEMPO spin label in unsaturated lipid (POPC and DOPC) bilayers at $T = 310$ K calculated using the CHARMM and AMBER force fields (the error bars denote estimated standard error). To see this figure in color, go online.

temperature (see Fig. S3). In light of the unsubstituted TEMPO partitioning to fluidic lipid phase and its exclusion from gel phase, the membrane phase-dependent behavior of the TEMPO-PC configuration, adopting the TEMPO-in (fluid phase) and TEMPO-out (gel phase) is not entirely unexpected.

- (2) Because the TEMPO moiety switches its location from the aqueous phase at low temperature ($T < T_m$) to the fluidic lipid phase at high temperature ($T > T_m$), the change in TEMPO mobility at $T \sim T_m$ would be not as discontinuous as 5-PC and 5-doxyl stearic acid (5-DSA) (8,19) or a hypothetical case of TEMPO being buried inside the bilayers over the entire temperature variation. This in part rationalizes the *absence* of a sharp (discontinuous) jump in the EPR-measured rotational diffusion rate and diffusivity of TEMPO across T_m (8,19) (see Fig. S3 as well).
- 3) The membrane phase-dependent location of TEMPO simultaneously rationalizes both the nitrogen hyperfine coupling constant data ($2A_z$) at $T = -165^\circ\text{C}$ (Fig. 8 B in (42)) and the oxygen transport parameter at $T = 25^\circ\text{C}$ (Fig. 9 B in (42)) for n -PC and TEMPO-PC in pure POPC bilayers by Subczynski et al. (42). Since the lipid phase transition temperature of pure POPC bilayers is $T_m = -2^\circ\text{C}$ (36), Subczynski et al.'s EPR signals and oxygen transport parameter data represent the data in the gel and fluid phases of POPC membranes, respectively. In (42), the former (EPR signals at $T = -165^\circ\text{C}$) suggested that TEMPO-PC is located in the more hydrophilic region, close to the water/lipid interface, than 5-PC or 7-PC, whereas the latter (oxygen transport parameter data at $T = 25^\circ\text{C}$) indicated that the TEMPO is in a lipophilic location comparable with the position of 5-PC.

These results, obtained at two different temperatures, compare well with the picture painted by our membrane phase-dependent location of the TEMPO moiety.

- 4) Our MD simulation results that show the location of TEMPO in fluid lipid bilayers below the level of phosphates are consistent with the previous studies obtained in joint refinement of the location of lipid-attached dyes by MD simulations and fluorescence quenching with lipid-attached TEMPO (13,14). In depth-dependent fluorescence quenching measurements with lipid-attached spin probes (18), an incorrectly interpreted transverse position of a TEMPO probe along the bilayer membrane could result in significant errors in determining the bilayer penetration of dye-labeled proteins.
- 5) A study by Raghuraman et al. (43), which employed red edge excitation shift and fluorescence measurements at varying temperatures across gel-to-fluid phase transition of DPPC bilayers, has indicated that acyl chain labeled NBD lipids (6- and 12-NBD-PC) tend to loop up in the fluid phase lipid, presumably driven by hydrogen bonding of the NBD group at membrane interface, whereas the NBD group in the gel phase remains in the deeper regions of the membranes. Although the membrane phase-dependent location of the NBD probe is opposite to the case of TEMPO, the effect of membrane phase state on the configuration of fluorescence probe is still there, highlighting the importance of assessing the physicochemical properties of lipids when carrying out spin probe measurements.
- 6) According to a recent experimental study by An et al. (44), sterol-derived Raman tags introduced in the lipid membrane exhibit head-in and head-out types of orientational dimorphism. It was shown that the head-out orientation was preferred when the terminal side chain attached to cholesterol was polar, and that, when a terminal side chain was incapable of making hydrogen bonds with water, the head-in configuration was favored at increased temperatures to minimize the perturbation to the lipid-water interface hydrogen bonding network (44), the situation of which is similar to the TEMPO spin label of the TEMPO-in configuration submerged in the lipid phase, as demonstrated in Fig. 2 B. The explanation based on the lipid-water hydrogen bond network, given for the orientational dimorphism of sterol-derived Raman tags, however, does not directly apply to the two alternative configurations of TEMPO-PC, given that the average number of H-bonds between TEMPO-PC and water molecules decreases, albeit in a minor way, from TEMPO-out to TEMPO-in configurations (Fig. S4). We surmise that gain in configurational entropy of the flexible headgroup and the nonpolar interaction between the TEMPO moiety and the lipid tail (Fig. 2 B) is the driving force that gives rise to the TEMPO-in configuration when lipid bilayers are in the fluid phase.

To recapitulate, despite some variations in the PMFs obtained for distinct lipid types and MD force fields (Figs. 3 and 4), our study using MD simulations carried out for single-component bilayer membranes leads to the conclusion that the location of the TEMPO moiety of TEMPO-PC in bilayers is membrane phase dependent, which we hope constructively addresses some of the issues discussed in the field (16,18,19). Finally, given that the membrane phase or membrane fluidity depends on a number of factors, such as temperature, types of fatty acids, presence of cholesterol, membrane curvature, medium osmolality, solutes in aqueous phase, and whether the measurement is made on single or multi-bilayer vesicle (4,28,45–50), extra attention should be paid to the physicochemical condition of bilayers when interpreting the data collected from TEMPO-PC.

SUPPORTING MATERIAL

Supporting material can be found online at <https://doi.org/10.1016/j.bpj.2022.05.044>.

AUTHOR CONTRIBUTIONS

C.H. designed the research. S.K. carried out all simulations. S.K. and C.H. analyzed the data and wrote the article.

ACKNOWLEDGMENTS

This work was supported by the KIAS Individual Grants CG080501 (to S.K.) and CG035003 (to C.H.). We thank the Center for Advanced Computation in KIAS for providing computing resources.

DECLARATION OF INTERESTS

The authors declare no competing interests.

REFERENCES

1. Freed, J. H., and G. K. Fraenkel. 1963. Theory of linewidths in electron spin resonance spectra. *J. Chem. Phys.* 39:326–348.
2. Seelig, J. 1971. Flexibility of hydrocarbon chains in lipid bilayers. *J. Am. Chem. Soc.* 93:5017–5022.
3. Klug, C. S., and J. B. Feix. 2008. Methods and applications of site-directed spin labeling EPR spectroscopy. *Methods Cell Biol.* 84:617–658.
4. Voinov, M. A., T. I. Smirnova, and A. I. Smirnov. 2022. EPR Oximetry with nitroxides: effects of molecular structure, pH, and electrolyte concentration. *Appl. Magn. Reson.* 53:247–264.
5. Chattopadhyay, A., and E. London. 1987. Parallax method for direct measurement of membrane penetration depth utilizing fluorescence quenching by spin-labeled phospholipids. *Biochemistry.* 26:39–45.
6. Brahma, R., and H. Raghuraman. 2022. Measuring membrane penetration depths and conformational changes in membrane peptides and proteins. *J. Membr. Biol.* 1–15. <https://doi.org/10.1007/s00232-022-00224-2>.
7. Armstrong, B. D., and S. Han. 2009. Overhauser dynamic nuclear polarization to study local water dynamics. *J. Am. Chem. Soc.* 131:4641–4647.
8. Kausik, R., and S. Han. 2009. Ultrasensitive detection of interfacial water diffusion on lipid vesicle surfaces at molecular length scales. *J. Am. Chem. Soc.* 131:18254–18256.
9. Cheng, C.-Y., J. Song, ..., S. Han. 2015. DMSO induces dehydration near lipid membrane surfaces. *Biophys. J.* 109:330–339.
10. Farahbakhsh, Z. T., C. Altenbach, and W. L. Hubbell. 1992. Spin labeled cysteines as sensors for protein-lipid interaction and conformation in rhodopsin. *Photochem. Photobiol.* 56:1019–1033.
11. Qin, Z., and D. S. Cafiso. 1996. Membrane structure of protein kinase C and calmodulin binding domain of myristoylated alanine rich C kinase substrate determined by site-directed spin labeling. *Biochemistry.* 35:2917–2925.
12. Seelig, J., and A. Seelig. 1980. Lipid conformation in model membranes and biological membranes. *Q. Rev. Biophys.* 13:19–61.
13. Kyrychenko, A., and A. S. Ladokhin. 2013. Molecular dynamics simulations of depth distribution of spin-labeled phospholipids within lipid bilayer. *J. Phys. Chem. B.* 117:5875–5885.
14. Kyrychenko, A., M. V. Rodnin, and A. S. Ladokhin. 2015. Calibration of distribution analysis of the depth of membrane penetration using simulations and depth-dependent fluorescence quenching. *J. Membr. Biol.* 248:583–594.
15. Faller, R. 2016. Molecular modeling of lipid probes and their influence on the membrane. *Biochim. Biophys. Acta Biomembr.* 1858:2353–2361.
16. Lee, Y., P. A. Pincus, and C. Hyeon. 2016. Effects of dimethyl sulfoxide on surface water near phospholipid bilayers. *Biophys. J.* 111:2481–2491.
17. Laudadio, E., R. Galeazzi, ..., P. Stipa. 2019. Depth distribution of spin-labeled liponitroxides within lipid bilayers: a combined EPR and molecular dynamics approach. *ACS Omega.* 4:5029–5037.
18. Kyrychenko, A., and A. S. Ladokhin. 2020. Location of TEMPO-PC in lipid bilayers: implications for fluorescence quenching. *J. Membr. Biol.* 253:73–77.
19. Schrader, A. M., and S. Han. 2017. Location of the TEMPO moiety of TEMPO-PC in lipid bilayers. *Biophys. J.* 113:966–969.
20. Sezer, D., J. H. Freed, and B. Roux. 2008. Parametrization, molecular dynamics simulation, and calculation of electron spin resonance spectra of a nitroxide spin label on a polyalanine α -helix. *J. Phys. Chem. B.* 112:5755–5767.
21. Klauda, J. B., R. M. Venable, ..., R. W. Pastor. 2010. Update of the CHARMM all-atom additive force field for lipids: validation on six lipid types. *J. Phys. Chem. B.* 114:7830–7843.
22. Lee, J., X. Cheng, ..., W. Im. 2016. CHARMM-GUI input generator for NAMD, GROMACS, AMBER, OpenMM, and CHARMM/OpenMM simulations using the CHARMM36 additive force field. *J. Chem. Theor. Comput.* 12:405–413.
23. Hess, B., C. Kutzner, ..., E. Lindahl. 2008. Gromacs 4: algorithms for highly efficient, load-balanced, and scalable molecular simulation. *J. Chem. Theor. Comput.* 4:435–447.
24. Bonomi, M. 2019. Promoting transparency and reproducibility in enhanced molecular simulations. *Nat. Methods.* 16:670–673.
25. Tribello, G. A., M. Bonomi, ..., G. Bussi. 2014. Plumed 2: new feathers for an old bird. *Comput. Phys. Commun.* 185:604–613.
26. Stendardo, E., A. Pedone, ..., V. Barone. 2010. Extension of the AMBER force-field for the study of large nitroxides in condensed phases: an ab initio parameterization. *Phys. Chem. Chem. Phys.* 12:11697–11709.
27. Nagle, J. F., and S. Tristram-Nagle. 2000. Structure of lipid bilayers. *Biochim. Biophys. Acta Biomembr.* 1469:159–195.
28. Nagle, J. F. 1980. Theory of the main lipid bilayer phase transition. *Annu. Rev. Phys. Chem.* 31:157–196.
29. Kusube, M., H. Matsuki, and S. Kaneshina. 2005. Thermotropic and barotropic phase transitions of N-methylated dipalmitoylphosphatidylethanolamine bilayers. *Biochim. Biophys. Acta Biomembr.* 1668:25–32.

30. Biltonen, R. L., and D. Lichtenberg. 1993. The use of differential scanning calorimetry as a tool to characterize liposome preparations. *Chem. Phys. Lipids*. 64:129–142.
31. Janiak, M. J., D. M. Small, and G. G. Shipley. 1979. Temperature and compositional dependence of the structure of hydrated dimyristoyl lecithin. *J. Biol. Chem.* 254:6068–6078.
32. Lis, L., D. McAlister, ..., V. Parsegian. 1982. Interactions between neutral phospholipid bilayer membranes. *Biophys. J.* 37:657–665.
33. Nagle, J. F., R. Zhang, ..., R. M. Suter. 1996. X-ray structure determination of fully hydrated L alpha phase dipalmitoylphosphatidylcholine bilayers. *Biophys. J.* 70:1419–1431.
34. Leekumjorn, S., and A. K. Sum. 2007. Molecular studies of the gel to liquid-crystalline phase transition for fully hydrated DPPC and DPPE bilayers. *Biochim. Biophys. Acta Biomembr.* 1768:354–365.
35. Koynova, R., and M. Caffrey. 1998. Phases and phase transitions of the phosphatidylcholines. *Biochim. Biophys. Acta Biomembr.* 1376:91–145.
36. Leekumjorn, S., and A. K. Sum. 2007. Molecular characterization of gel and liquid-crystalline structures of fully hydrated POPC and POPE bilayers. *J. Phys. Chem. B.* 111:6026–6033.
37. Ulrich, A. S., M. Sami, and A. Watts. 1994. Hydration of DOPC bilayers by differential scanning calorimetry. *Biochim. Biophys. Acta Biomembr.* 1191:225–230.
38. McConnell, H. M., K. L. Wright, and B. G. McFarland. 1972. The fraction of the lipid in a biological membrane that is in a fluid state: a spin label assay. *Biochem. Biophys. Res. Commun.* 47:273–281.
39. Marsh, D., A. Watts, and P. F. Knowles. 1976. Evidence for phase boundary lipid. Permeability of Tempo-choline into dimyristoylphosphatidylcholine vesicles at the phase transition. *Biochemistry.* 15:3570–3578.
40. Shimshick, E. J., and H. M. McConnell. 1973. Lateral phase separation in phospholipid membranes. *Biochemistry.* 12:2351–2360.
41. Shimshick, E. J., and H. M. McConnell. 1973. Lateral phase separations in binary mixtures of cholesterol and phospholipids. *Biochem. Biophys. Res. Commun.* 53:446–451.
42. Subczynski, W. K., M. Raguz, and J. Widomska. 2010. Studying lipid organization in biological membranes using liposomes and EPR spin labeling. *In Liposomes.* Springer, pp. 247–269.
43. Raghuraman, H., S. Shrivastava, and A. Chattopadhyay. 2007. Monitoring the looping up of acyl chain labeled NBD lipids in membranes as a function of membrane phase state. *Biochim. Biophys. Acta Biomembr.* 1768:1258–1267.
44. An, X., A. Majumder, ..., B. M. Reinhard. 2021. Interfacial hydration determines orientational and functional dimorphism of sterol-derived Raman tags in lipid-coated nanoparticles. *Proc. Natl. Acad. Sci. U S A.* 118.
45. Marsh, D., A. Watts, and P. Knowles. 1977. Cooperativity of the phase transition in single- and multibilayer lipid vesicles. *Biochim. Biophys. Acta Biomembr.* 465:500–514.
46. Kusumi, A., W. K. Subczynski, ..., H. Merkle. 1986. Spin-label studies on phosphatidylcholine-cholesterol membranes: effects of alkyl chain length and unsaturation in the fluid phase. *Biochim. Biophys. Acta Biomembr.* 854:307–317.
47. Ipsen, J. H., G. Karlström, ..., M. Zuckermann. 1987. Phase equilibria in the phosphatidylcholine-cholesterol system. *Biochim. Biophys. Acta Biomembr.* 905:162–172.
48. Shin, Y., and J. H. Freed. 1989. Dynamic imaging of lateral diffusion by electron spin resonance and study of rotational dynamics in model membranes. Effect of cholesterol. *Biophys. J.* 55:537–550.
49. Anderson, N. A., L. J. Richter, ..., K. A. Briggman. 2006. Determination of lipid phase transition temperatures in hybrid bilayer membranes. *Langmuir.* 22:8333–8336.
50. Chakraborty, S., M. Doktorova, ..., M. F. Brown. 2020. How cholesterol stiffens unsaturated lipid membranes. *Proc. Natl. Acad. Sci. U S A.* 117:21896–21905.

Biophysical Journal, Volume 121

Supplemental information

Location of the TEMPO moiety of TEMPO-PC in phosphatidylcholine bi-layers is membrane phase dependent

Seonghoon Kim and Changbong Hyeon

Supporting Information: Location of the TEMPO moiety of TEMPO-PC in phosphatidylcholine bilayers is membrane phase-dependent

Seonghoon Kim¹ and Changbong Hyeon^{1,*}

¹School of Computational Sciences, Korea Institute for Advanced Study, Seoul 02455, Korea

*Correspondence: hyeoncb@kias.re.kr

SUPPLEMENTARY FIGURES

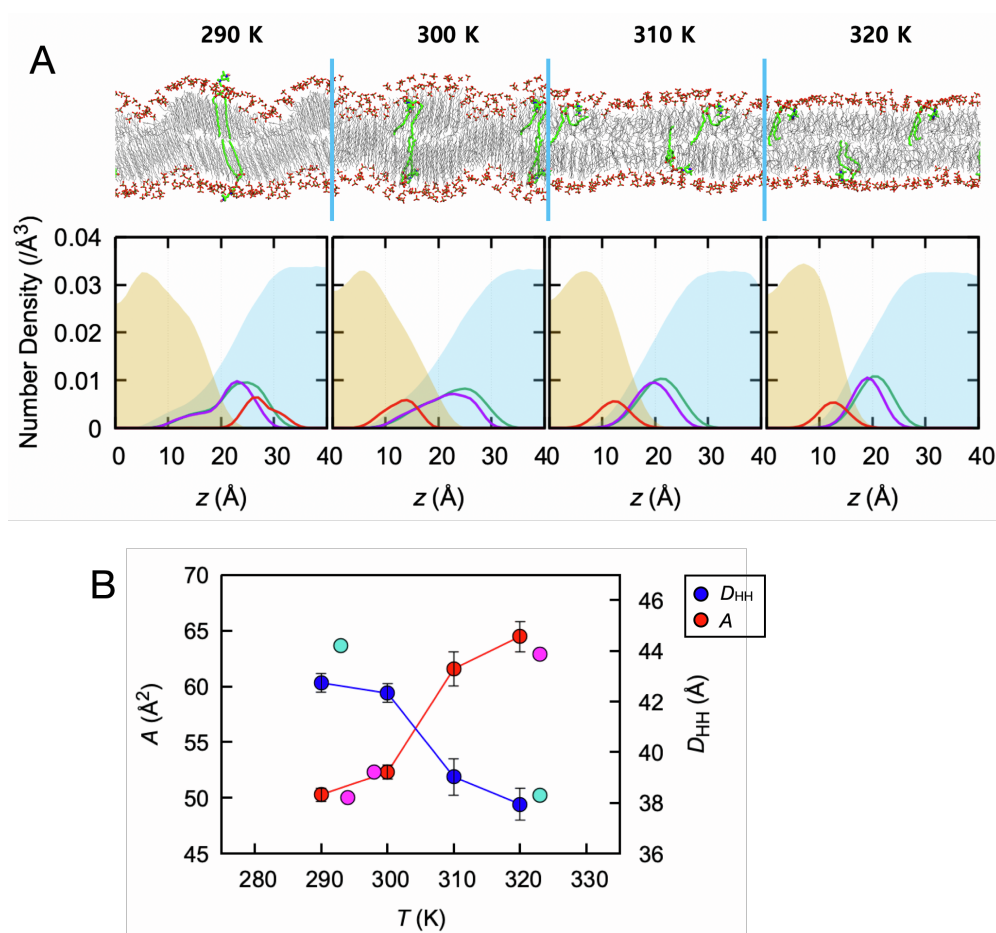


Figure S1: **A.** Snapshots of TEMPO-PC configurations in DPPC bilayers (first row). The density profiles of the heavy atoms shown in the second row. Details of the depiction are the same as Fig.1 but the calculation was carried out with AMBER LIPID17 force field. **B.** Area per lipid (A) and bilayer thickness (D_{HH}) of DPPC bilayers obtained from MD simulations with AMBER LIPID17 force field at varying temperatures (error bars denote the standard deviation). The filled circles in magenta and cyan represent the experimental measurements for A and D_{HH} , respectively.

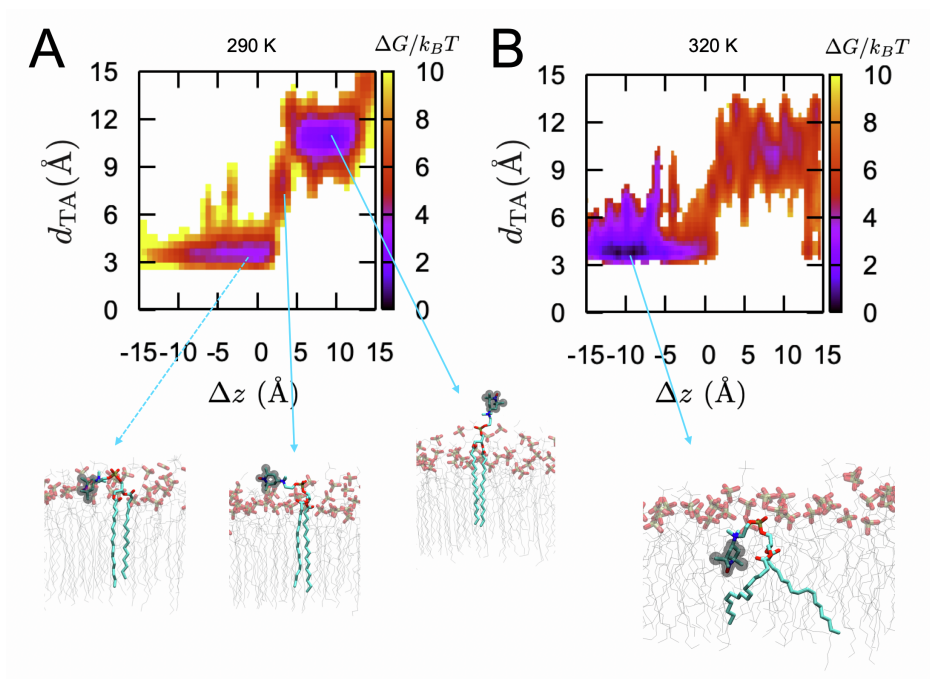


Figure S2: 2D PMF of TEMPO spin label in the DPPC bilayers calculated as a function of Δz (height difference between nitroxide oxygen and phosphorus atoms) and d_{TA} (minimal distance between any heavy atom of TEMPO and C2-C5 of acyl chain at (A) $T (= 290 \text{ K}) < T_m$ and $T (= 320 \text{ K}) > T_m$). The calculation was carried out under CHARMM36.

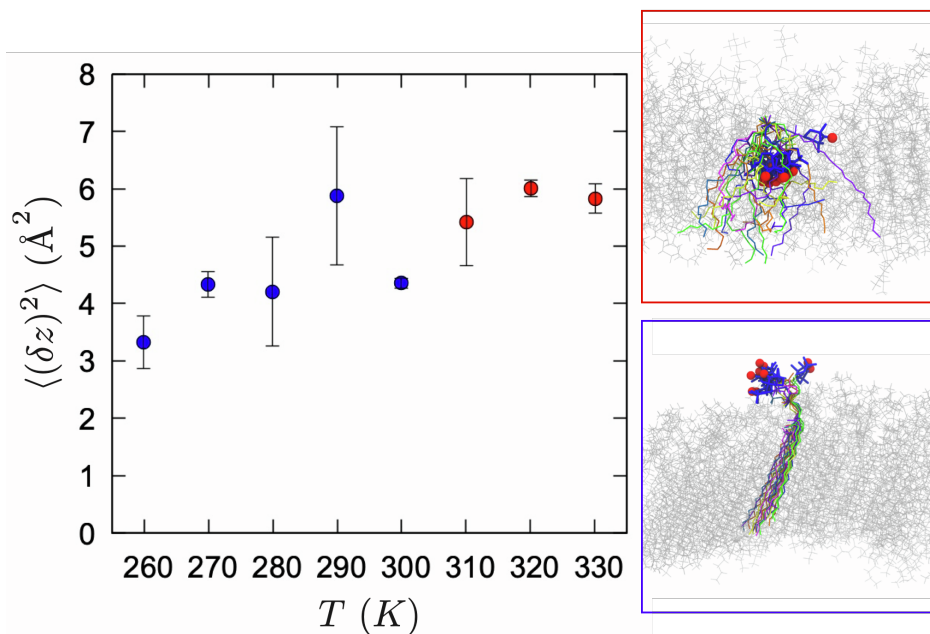


Figure S3: Fluctuations of TEMPO perpendicular to the bilayer plane, $\langle (\delta z)^2 \rangle$ (variances in the z -component of the nitroxide oxygen coordinate), as a function of temperature calculated based on the MD simulation trajectories used to generate the density profiles shown in Fig. 1A. The values of $\langle (\delta z)^2 \rangle$ in red ($T > T_m = 314 \text{ K}$) and in blue ($T < T_m$) in the main panel on the left are calculated by using only TEMPO-in and TEMPO-out configurations, respectively. Two panels on the right depicts the extent of fluctuations in the TEMPO-in at 320 K (red box) and TEMPO-out configurations at 280 K (blue box).

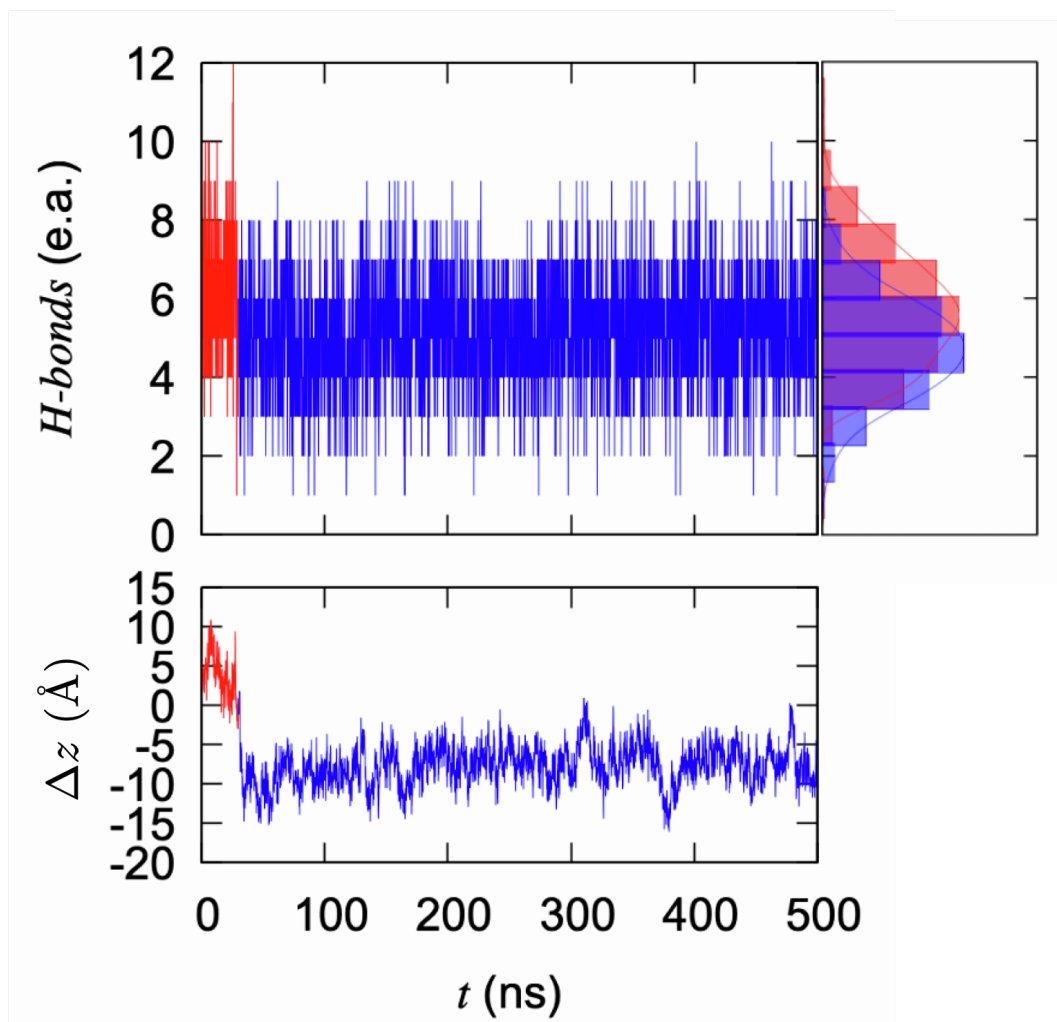


Figure S4: Number of hydrogen bonds between TEMPO-PC and water molecules for the simulation performed at $T = 320$ K. The TEMPO-PC switches its configuration from TEMPO-out ($\Delta z > 0$, red) to TEMPO-in ($\Delta z < 0$, blue) at $t \approx 30$ ns. Upon this change, the number of H-bonds decreases from ~ 6 to ~ 5 .